Molecular Biology of the Cell
Vol. 20, 5181–5194, December 15, 2009

MICAL-L1 Links EHD1 to Tubular Recycling Endosomes and Regulates Receptor Recycling

Mahak Sharma, Sai Srinivas Panapakkam Giridharan, Juliati Rahajeng, Naava Naslavsky, and Steve Caplan

Department of Biochemistry and Molecular Biology and Eppley Cancer Center, University of Nebraska Medical Center, Omaha, NE 68198-5870

Submitted June 30, 2009; Revised October 8, 2009; Accepted October 19, 2009
Monitoring Editor: Sandra L. Schmid

Endocytic recycling of receptors and lipids occurs via a complex network of tubular and vesicular membranes. EHD1 is a key regulator of endocytosis and associates with tubular membranes to facilitate recycling. Although EHD proteins tubulate membranes in vitro, EHD1 primarily associates with preexisting tubules in vivo. How EHD1 is recruited to these tubular endosomes remains unclear. We have determined that the Rab8-interacting protein, MICAL-L1, associates with EHD1, with both proteins colocalizing to long tubular membranes, in vitro and in live cells. MICAL-L1 is a largely uncharacterized member of the MICAL-family of proteins that uniquely contains two asparagine-proline-phenylalanine motifs, sequences that typically interact with EH-domains. Our data show that the MICAL-L1 C-terminal coiled-coil region is necessary and sufficient for its localization to tubular membranes. Moreover, we provide unexpected evidence that endogenous MICAL-L1 can link both EHD1 and Rab8a to these structures, as its depletion leads to loss of the EHD1-Rab8a interaction and the absence of both of these proteins from the membrane tubules. Finally, we demonstrate that MICAL-L1 is essential for efficient endocytic recycling. These data implicate MICAL-L1 as an unusual type of Rab effector that regulates endocytic recycling by recruiting and linking EHD1 and Rab8a on membrane tubules.

INTRODUCTION

The process of internalizing proteins and lipids from the plasma membrane is a critical event for eukaryotic cells. Internalization is facilitated by a wide range of regulatory proteins and occurs by a variety of well-characterized mechanisms, including via clathrin-coated pits, independently of clathrin, through caveolae and by various pinocytic pathways (Conner and Schmid, 2003; Mayor and Pagano, 2007). On internalization via clathrin-dependent and -independent mechanisms, vesicles derived from the plasma membrane fuse with one another and internalized proteins converge at the early endosome (Naslavsky *et al.*, 2003). From this sorting station, many receptors are transported to the late endosomal/lysosomal pathway for degradation. Other receptors, however, are not degraded, but are returned to the plasma membrane either directly from early endosomes in a rapid process known as "fast recycling," or indirectly via a "slow-recycling" process (Maxfield and McGraw, 2004). Slow recycling depends on a series of tubular and vesicular membrane structures that emanate from the region of the microtubule-organizing center and are collectively known as the endocytic recycling compartment (ERC; Hopkins, 1983; Maxfield and McGraw, 2004).

The Rab family of small GTP-binding proteins and their effectors play key roles in the regulation of endocytic trafficking and recycling to the plasma membrane (Pfeffer and Aivazian, 2004; Grosshans *et al.*, 2006). Endocytic activity is also regulated by the C-terminal Eps15 homology domain (EHD) family of proteins (reviewed in Grant and Caplan, 2008). The single worm EHD orthologue was originally identified by genetic screen of *Caenorhabditis elegans* endocytic mutants and is known as RME-1 (Grant *et al.*, 2001). In mammalian cells, however, there are four highly homologous paralogues of the EHD family (EHD1-4), which carry out distinct, but partially overlapping functions in endocytic trafficking (Naslavsky and Caplan, 2005; Grant and Caplan, 2008). EHD1, arguably the best characterized EHD protein, has a primary role in the regulation of endocytic trafficking from the ERC to the plasma membrane (Grant *et al.*, 2001; Lin *et al.*, 2001; Caplan *et al.*, 2002; Naslavsky *et al.*, 2004; Rapaport *et al.*, 2006). Although EHD proteins display similarities to the GTP-binding Ras family of proteins (Caplan *et al.*, 2002; Daumke *et al.*, 2007), they bind and hydrolyze ATP (Lee *et al.*, 2005; Naslavsky *et al.*, 2006; Daumke *et al.*, 2007). Indeed, ATP binding appears to be a requirement for the localization of EHD1 to its unique array of tubular and vesicular membranes and the ability of EHD proteins to oligomerize (Caplan *et al.*, 2002; Naslavsky *et al.*, 2006; Daumke *et al.*, 2007). In addition to their propensity to oligomerize, EHD proteins bind to Rab effectors to coordinate activity with Rab-family proteins. For example, EHD1 interacts with the Rab4/5 divalent effector, Rabenosyn-5 (Naslavsky *et al.*, 2004), whereas EHD1 and EHD3 interact with the Rab11 effector, Rab11-FIP2 (Naslavsky *et al.*, 2006). Both of these interactions are mediated through the EH-domain and multiple asparagine-proline-phenylalanine (NPF) motifs in Rabenosyn-5 and Rab11-FIP2 (Naslavsky *et al.*, 2004; Naslavsky *et al.*, 2006). Thus Rab family proteins and EHDs provide a network of endocytic regulation that is bridged by common "effectors."

This article was published online ahead of print in *MBC in Press* (http://www.molbiolcell.org/cgi/doi/10.1091/mbc.E09–06–0535) on October 28, 2009.

Address correspondence to: Steve Caplan (scaplan@unmc.edu) or Naava Naslavsky (nnaslavsky@unmc.edu).

A trademark characteristic of EHD1 is its distribution to long tubular membranes and vesicles that generally emanate from the ERC (Caplan *et al.*, 2002). Recent studies demonstrate that cells exhibit impaired recycling when expressing EHD1 with an amino acid substitution that renders it incapable of tubule association, consistent with a requirement for EHD1-tubule association for efficient recycling (Jovic *et al.*, 2009). However, the issue of whether EHD proteins intrinsically tubulate membranes or whether they associate with preexisting tubular structures has been difficult to assess. In vitro, purified EHD2 can clearly deform lipids into tubular structures (Daumke *et al.*, 2007). In vivo, however, marker proteins that colocalize with EHD1 tubules, including Rab8a (Roland *et al.*, 2007), continue to associate with these structures upon EHD1 depletion, suggesting that EHD1 is not required for their formation or maintenance (Jovic *et al.*, 2009). In this study, we have hypothesized that a yet-to-be-identified interacting protein is likely responsible for EHD1 recruitment to tubular membranes. We therefore initiated a screen and identified MICAL-Like 1 (MICAL-L1) as a novel EHD1 interaction partner involved in the recruitment of EHD1 to tubular ERC membranes. Our data implicate MICAL-L1 as a novel regulator of endocytic recycling and support the unique notion that effector proteins such as MICAL-L1 can act upstream of Rab proteins and link EHD1 and Rab8a to tubular ERC membranes.

MATERIALS AND METHODS

Recombinant DNA Constructs

Cloning of full-length wild-type (WT) Myc-EHD1, Myc-EHD1 ΔEH, Myc-EHD1K483E, Myc-EHD2, Myc-EHD3, HA-EHD4, glutathione *S*-transferase (GST)-EH domain of EHD1, and GST-EH domain of EHD4 have been described previously (Caplan *et al.*, 2002; Naslavsky *et al.*, 2004, 2006, 2007; Sharma *et al.*, 2008). EH domains of EHD2 and EHD3 were subcloned into the GST fusion bacterial expression vector pGEX-6P-2 (GE Life Sciences, Piscataway, NJ). Tomato EHD1 was subcloned into the ptd-tomato C1 vector (Clontech, Palo Alto, CA). A human MICAL-L1 cDNA clone was purchased from ATCC (Manassas, VA) and subcloned into EGFP-C3 (Clontech) and pCDNA 3.1(−) expression vectors (Invitrogen, Carlsbad, CA) using standard procedures. GST-EH1K483E, Myc-EHD1 K483E + W485A, GFP-MICAL-L1 ΔNPF, and deletion mutants were generated using the QuickChange site-directed mutagenesis kit (Stratagene, La Jolla, CA). siRNA-resistant hemagglutinin (HA)-MICAL-L1 and siRNA-resistant HA-WT coiled-coil (CC) only was created similarly, generating cDNA mutations in the oligonucleotide-binding region. HA-MICAL-L1 (672–863) and HA-MICAL-L1 (700–863) were generated by PCR amplification and cloned into pcDNA 3.1(−). Two-hybrid control vectors (GAL4ad–SV40 large T-antigen and GAL4bd–p53) were obtained from Clontech. pGADT7 two-hybrid vectors containing EHD1 have been described previously (Naslavsky *et al.*, 2004). WT MICAL-L1, ΔNPF mutants, and site 1, site 2, and site 1 + 2 mutants were cloned into the pGBKT7 and pGADT7 vectors. All constructs were sequence verified and transfected using Fugene or FugeneHD (Roche Applied Science, Indianapolis, IN). The Cherry-Rab8a, Rab8a-WT, Rab8aQ67L, and Rab8aT22N constructs in yeast two-hybrid vectors were a kind gift from Dr. J. Goldenring (Vanderbilt Ingram Cancer Center, TN). Green fluorescent protein (GFP)-H-Ras (GFP fused to the double palmitoylated and farnesylated carboxy terminal tail of H-Ras) was kindly provided by Dr. J. Donaldson (NIH).

Antibodies and Reagents

The following antibodies were used in this study: rabbit polyclonal antibodies against EHD1 and against EHD4 (Naslavsky *et al.*, 2004; Sharma *et al.*, 2008); mouse anti-MICAL-L1 antibodies (Novus Biologicals, Littleton, CO); rabbit antibodies against Myc epitope (Santa Cruz Biotechnology, Santa Cruz, CA) and against Rab11 (US Biologicals, Swampscott, MA); mouse monoclonal antibodies directed against the HA epitope (Covance, Princeton, NJ) and against GFP epitope (Roche Diagnostics, Indianapolis, IN); mouse anti-EEA1, anti-Rab8, and anti-cytochrome C (BD Biosciences, San Jose, CA); mouse anti-transferrin (Tf) receptor (Zymed, San Francisco, CA); mouse anti-β1 integrin antibody (Serotec, Raleigh, NC); and mouse anti-actin (Abcam, Cambridge, MA). Secondary donkey anti-mouse Alexa 488, goat anti-mouse Alexa 568, goat anti-rabbit Alexa 488, and goat anti-rabbit Alexa 568 antibodies were purchased from Invitrogen. Goat anti-mouse horseradish peroxidase (HRP) was obtained from Jackson ImmunoResearch Laboratories (West Grove, PA). Donkey anti-rabbit HRP was obtained from GE Life Sciences. Tf-Alexa Fluor 568 (Tf-568) was purchased from Invitrogen.

Membrane Fractionation, Immunoprecipitations, and GST Pulldowns

The GST-EH1, GST-EH1K483E, GST-EH2, GST-EH3, and GST-EH4 fusion protein was purified by standard methods and bound to either GST beads (see Figures 1 and 3 and Supplemental Figure S1) or anti-GST antibody coupled to protein G beads (see Figure 6) for 2 h. Untransfected and transfected HeLa cell lysates prepared either in 0.5% CHAPS buffer (Figure 1) or 1% Brij98 buffer containing GTPγS (Figure 6) was incubated with purified bound GST proteins for 2 h, followed by washes with PBS or PBS containing GTPγS (Figure 6). Eluted proteins were resolved as described below and immunoblotted with appropriate antibodies. Enhanced chemiluminescence (ECL) was used for detection. Membrane and cytosol fractionation was done as described previously (Sharma *et al.*, 2008). For immunoprecipitations, cells were lysed for 1 h in buffer containing 25 mM Tris-HCl, pH 7.4, 125 mM NaCl, 1 mM $MgCl_2$, 1% Brij98 (wt/vol), 0.25 mM AEBSF, 10 μM leupeptin, and 10 μM aprotinin. Lysates were immunoprecipitated with goat anti-HA antibody-conjugated agarose beads (Bethyl Laboratories, Montgomery, TX). After 14 h at 4°C, immunoprecipitates were washed and eluted by 125 mM Tris, pH 6.8, 2% SDS, and 12% glycerol at 95°C. Densitometric analysis of the immunoblots was utilized to calculate the intensity of protein bands on the immunoblots by subtracting the mean luminosity of the protein band from background and multiplying the mean of luminosity by number of pixels as measured by Adobe Photoshop software (San Jose, CA).

Yeast Two-Hybrid Analysis

The yeast two-hybrid assay was done as described previously (Naslavsky *et al.*, 2004). Briefly, the *Saccharomyces cerevisiae* strain AH109 (BD Biosciences Clontech, Palo Alto, CA) was maintained on YPD agar plates. Transformation was done by the lithium acetate procedure as described in the instructions for the MATCHMAKER two-hybrid kit (BD Biosciences Clontech). For colony growth assays, AH109 cotransformants were streaked on plates lacking leucine and tryptophan and allowed to grow at 30°C, usually for 3 d or until colonies were large enough for further assays. An average of three to four colonies was then chosen and suspended in water, equilibrated to the same optical density at 600 nm, and replated on plates lacking leucine and tryptophan (+HIS) as well as plates also lacking histidine (−HIS).

Gene Knockdown by siRNA and Rescue Using siRNA-resistant MICAL-L1 Expression

siRNA duplexes for EHD1, EHD3, and EHD4 (synthesized by Dharmacon, Lafayette, CO) were transfected using Dharmafect (Dharmacon) as previously described (Naslavsky *et al.*, 2006; Sharma *et al.*, 2008) for 72 h. On-Target SMART pool from Dharmacon was used for MICAL-L1 and Rab8a. The siRNA-resistant rescue constructs of MICAL-L1 was transfected using FuGENE HD (Roche).

Immunofluorescence and Tf and β1 Integrin Uptake Assays

Immunofluorescence staining was carried out as described previously (Naslavsky *et al.*, 2006). All images were acquired using a Zeiss LSM 5 Pascal confocal microscope (Carl Zeiss, Thornwood, NY), using a Zeiss 63× 1.4 NA oil objective with appropriate filters. Fluorochromes are listed in *Antibodies and Reagents* above. The LSM 5 Pascal software was used for data acquisition; linear adjustments (contrast and brightness) were done with Adobe Photoshop. Tf and β1 integrin pulse-chase assays were done as described previously (Jovic *et al.*, 2009). Quantification of mean fluorescence was done using LSM Pascal software. The mean ± SE was calculated from counting 70–80 cells each from three independent experiments (see bars on figures).

Live Imaging by Time-Lapse Fluorescence Microscopy

HeLa cells seeded on a Lab-Tek chambered coverglass system (Nunc, Rochester, NY) were transfected with plasmids encoding either GFP–MICAL-L1 alone or both GFP-MICAL-L1 and Tomato-EHD1. Twenty hours after transfection, live images of the GFP- and Tomato-expressing cells were obtained a Zeiss LSM 5 Pascal confocal microscope (Zeiss). Temperature was maintained at 37°C with a water heated stage and lens warmer (Zeiss). The laser excitation setting was maintained at 488 nm for GFP and 543 nm for tomato, with emission detected by appropriate filter sets as supplied by the manufacturer. For live Tf pulse chase, GFP-MICAL-L1–transfected cells were starved for 30 min followed by a 10-min pulse of Tf-568. Cells were then washed with PBS followed by incubation in complete media while imaging of internalized Tf and GFP-MICAL-L1 was done for the indicated times. For fluorescence recovery studies, selective photobleaching was performed with the 488- and 543-nm laser line at full power, and recovery was then monitored at low intensity illumination for the times indicated. Image acquisition, data collection, and image processing were performed using LSM 5 Pascal and ImageJ software (available at http://rsb.info.nih.gov/ij/download/).

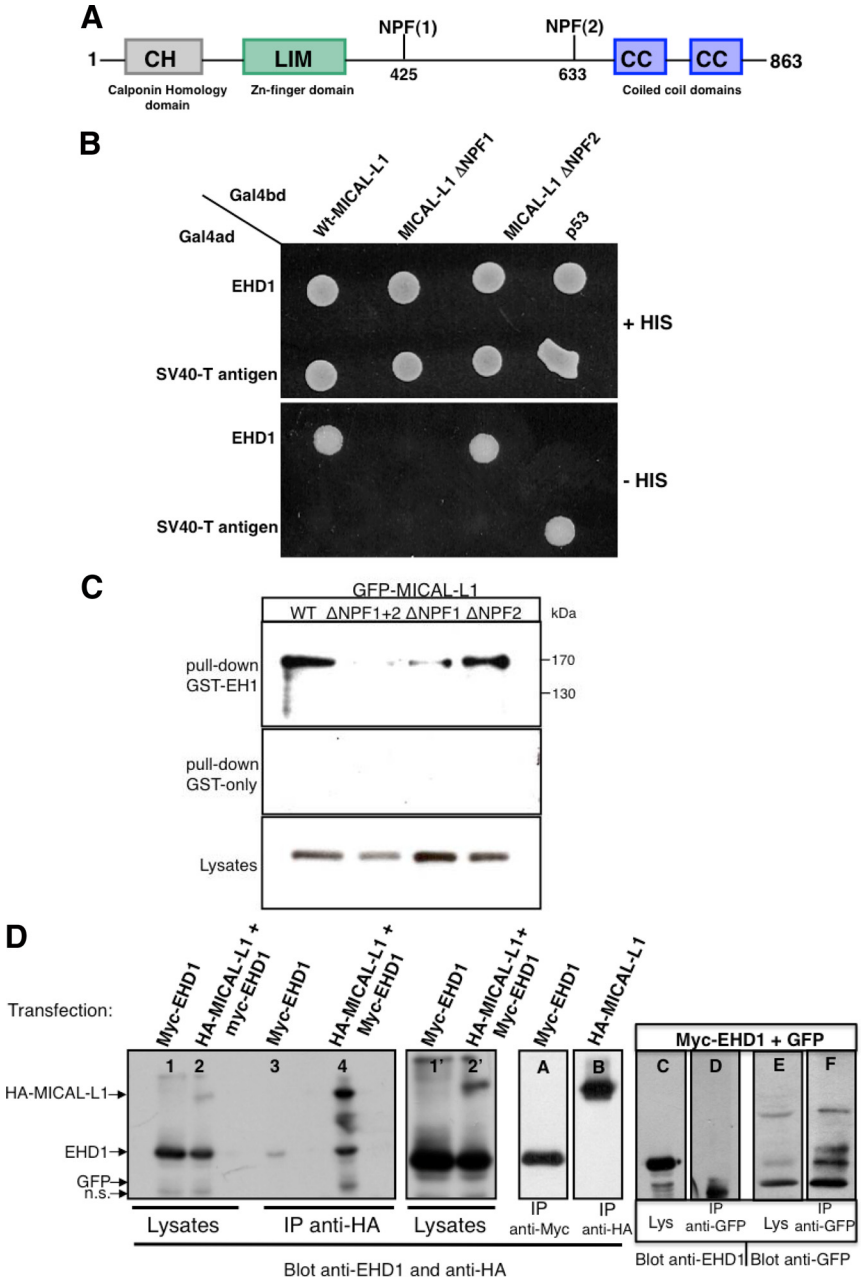

Figure 1. MICAL-L1 interacts with EHD1 via the first of its two NPF motifs. (A) Schematic representation of MICAL-L1 domain organization. MICAL-L1 contains an N-terminal calponin homology (CH) domain; a Lin11, Isl-1, Mec-3 (LIM) domain; two NPF motifs; and two C-terminal coiled-coil (CC) domains. (B) The *S. cerevisiae* yeast strain AH109 was cotransformed with the indicated GAL4-binding domain (GAL4bd) fusion constructs and Galbd-p53 (control), together with the indicated GAL4 transcription activation (GAL4ad) fusion products: Gal4ad-EHD1 or GAL4ad-SV40 large T-antigen (control). Cotransformants were assayed for their growth on nonselective (+HIS) and selective (−HIS) media. (C) Bacterially expressed, purified recombinant GST-EH-domain of EHD1 (top; GST-EH1) or GST-only (middle) was incubated with lysates from HeLa cells transfected with either WT GFP-MICAL-L1 (WT), GFP-MICAL-L1 with both NPF motifs mutated (ΔNPF1+ΔNPF2), GFP-MICAL-L1 with the first NPF motif mutated (ΔNPF1), or GFP-MICAL-L1 with the second NPF motif mutated (ΔNPF2). The bound proteins were resolved by 8% reducing SDS-PAGE, transferred to nitrocellulose, and immunoblotted with mouse anti-GFP, followed by anti-mouse HRP-conjugated antibodies. ECL was used for detection, and 6% of the total input is shown in the bottom panel. (D) HeLa cells were either transfected with Myc-EHD1 alone (lanes 1, 3, and A) or HA-MICAL-L1 alone (lane B) or cotransfected either with HA-MICAL-L1 and Myc-EHD1 (lanes 2 and 4) or GFP and Myc-EHD1 (lanes C–F). After 48 h, cells were lysed and subjected to immunoprecipitations with anti-HA antibody-conjugated agarose beads (lanes 3, 4, and B), with anti-Myc antibodies (lane A), or with anti-GFP antibodies (lanes D and F). Immunoprecipitates and total cell lysates (as indicated) were resolved by 8% nonreducing SDS-PAGE, transferred to nitrocellulose, and immunoblotted with anti-EHD1, anti-HA, and anti-GFP antibodies followed by detection with anti-rabbit and anti-mouse HRP-conjugated antibodies. ECL was used for detection. Lanes 1′ and 2′ show longer exposures of lanes 1 and 2, and 2% of the total input was loaded in lanes 1, 2, C, and E.

RESULTS

MICAL-L1 Interacts with EHD1 via Its First NPF Motif

To identify functional interacting proteins that might aid EHD1 in its regulatory role in recycling, we expressed the EH domain of EHD1 as a GST-fusion protein and used it as bait in pulldown assays with bovine brain cytosol. Mass spectrometry analysis (LC-MS/MS) of tryptic peptides resulted in the isolation of several peptides matching the sequence of MICAL-Like 1 (MICAL-L1), a member of the molecule interacting with CasL (MICAL) family of proteins with a molecular mass of ~130 kDa. As shown (Figure 1A) MICAL-L1 contains an N-terminal calponin homology (CH) domain found in actin-binding proteins; an Lin11, Isl-1, Mec-3 (LIM) domain, which comprises two contiguous zinc finger domains and is involved in cytoskeletal organization; two NPF motifs (sequences that frequently allow binding to EH-domains); and a C-terminal region containing two CCs.

Using yeast two-hybrid binding assays, we confirmed the association of EHD1 with WT MICAL-L1 (Figure 1B). Mutation of the first NPF motif to APA (MICAL-L1 ΔNPF1), but not the second one (MICAL-L1 ΔNPF2), invoked a loss of MICAL-L1 interaction with EHD1 (Figure 1B). Moreover, when cells were transfected with either GFP-tagged WT MICAL-L1 or MICAL-L1 bearing mutations in only the second NPF motif (ΔNPF2), MICAL-L1 could be pulled down by GST fused to the EH domain of EHD1 (GST-EH1; Figure 1C). On the other hand, when GFP-MICAL-L1 with mutations in its first NPF motif (ΔNPF1) or GFP-MICAL-L1 with mutations in both NPF motifs (ΔNPF1 + 2) was expressed, dramatically reduced levels were precipitated by GST-EH1 (Figure 1C). These findings indicate a specific requirement

for the first MICAL-L1 NPF motif for binding to EHD1. To verify the significance of these interactions in vivo, we initiated coimmunoprecipitations. Cells were transfected either with Myc-EHD1 alone or cotransfected with Myc-EHD1 and HA-MICAL-L1 (Figure 1D). Overall expressed protein levels in the lysates were assessed by immunoblot analysis (Figure 1D, lanes 1 and 2, and longer exposure in lanes 1′ and 2′), and direct pulldowns of Myc-EHD1 and MICAL-L1 were confirmed (lanes A and B). As we predicted on the basis of the yeast two-hybrid binding studies, WT HA-MICAL-L1 immunoprecipitated EHD1 from the cotransfected cell lysates (Figure 1D, lane 4). As a control, we observed very little nonspecific binding of EHD1 with the antibody coated beads (Figure 1D, lane 3). Additionally, when cells were cotransfected with Myc-EHD1 and GFP vector alone, although both EHD1 and GFP could be observed in the lysate (Figure 1D, lanes C and E), and when the immunoprecipitation of GFP itself was successful (Figure 1D, lanes E and F), no EHD1 was observed coimmunoprecipitating with the GFP control (Figure 1D, lane D). These data clearly demonstrate that EHD1 interacts with MICAL-L1 in vivo.

Because EHD1 displays a significant level of homology with its paralogs, EHD2, EHD3, and EHD4, we next tested the ability of MICAL-L1 to interact with these EHD proteins. Selective two-hybrid binding analysis revealed that although EHD1 and EHD3 (the closest EHD1 paralog) both could interact with MICAL-L1, little or no binding was detected between MICAL-L1 and either EHD2 or EHD4 (Supplemental Figure S1A). In addition, MICAL-L1 did not display a significant level of homo-oligomerization. We then confirmed these findings by doing GST-pulldown assays, utilizing the GST-fused EH domains of EHD1-4 as bait (with GST-alone as a negative control). As demonstrated (Supplemental Figure S1B), similar levels of all five GST proteins were utilized to bind to endogenous MICAL-L1 from HeLa cell lysates, and the EH-domains of EHD1 and EHD3 showed significant binding. In this assay, the isolated EH-domain of EHD4 was also able to interact moderately with MICAL-L1, although the EH-domain of EHD2 again did not bind to MICAL-L1.

MICAL-L1 and EHD1 Are Highly Colocalized on Tubular Membranes

On the basis of the newly discovered interaction between MICAL-L1 and EHD1, we predicted that MICAL-L1 might also associate with tubular membranes. To determine the localization of MICAL-L1 in HeLa cells and whether MICAL-L1 and EHD1 colocalize, Myc–EHD1 and HA-MICAL-L1 were cotransfected and stained with anti-Myc and anti-HA antibodies (Figure 2, A–C). MICAL-L1 displayed a remarkable distribution to an array of tubular (and some vesicular) membranes and overlapped extensively with EHD1. To rule out potential artifacts due to overexpression, we also analyzed the subcellular localization of MICAL-L1 and EHD1 using specific antibodies that recognize the endogenous proteins (Figure 2, D–F). Endogenous MICAL-L1 showed a very similar subcellular distribution pattern to that of the overexpressed protein, colocalizing with endogenous EHD1 on tubular membranes, although the level of tubular-associated endogenous EHD1 was significantly less than that of the endogenous MICAL-L1.

To better understand the dynamics of EHD1 and MICAL-L1 localization to tubular membranes, we performed fluorescence recovery after photobleaching (FRAP) experiments (Supplemental Figure S2 and Supplemental Video 1). Live cells expressing Tomato-EHD1 and GFP-MICAL-L1 were imaged every 10 s by dual channel time-lapse confocal microscopy. A region of interest (boxed region and inset) with two independent tubules decorated by both GFP-MICAL-L1 and Tomato-EHD1 were photobleached by high laser intensity, and the "recovery" or return of the fluorescence signal to these structures were monitored over time. As demonstrated, the simultaneous recruitment of MICAL-L1 and EHD1 to these membranes (most likely from the cytoplasm) was first observed within 3 min of the photobleach and reached >50% of the original level of fluorescence under 5 min. Moreover, some of the shorter EHD1- and MICAL-L1–decorated tubules displayed dynamic movement, with smaller structures that could be observed fusing with one another and potentially undergoing fission-like processes (see Supplemental Video 2). These data indicate that both MICAL-L1 and EHD1 are dynamically recruited to tubular membranes with similar kinetics and that the tubules themselves are capable of dynamic movement within the cells.

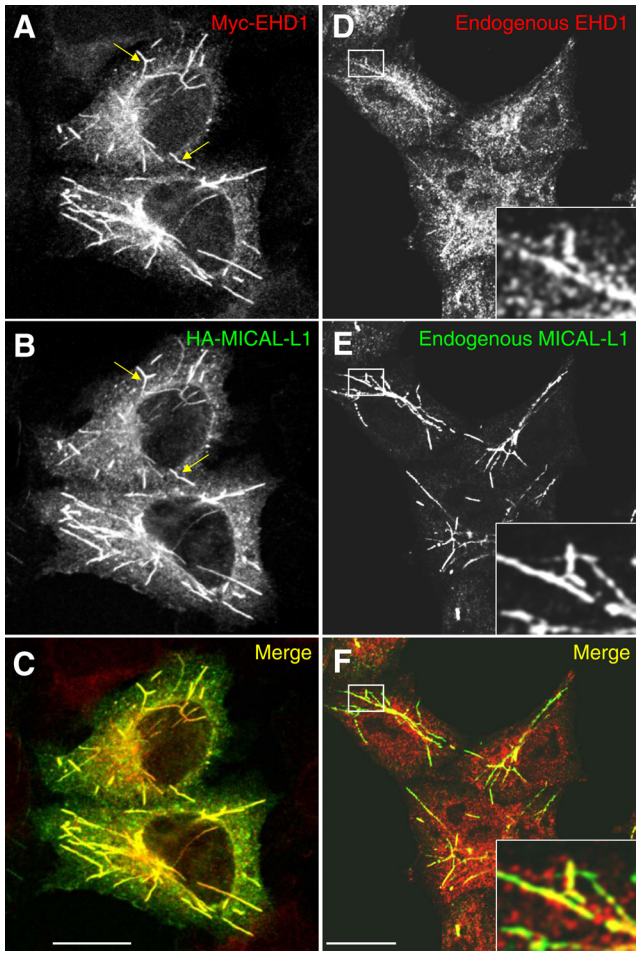

Figure 2. MICAL-L1 colocalizes with EHD1 on tubular endosomes. (A–C) HeLa cells on coverslips were transiently cotransfected with Myc-EHD1 and HA-MICAL-L1. After 24 h, cells were fixed and incubated with rabbit anti-Myc and mouse anti-HA antibodies. After washing, cells were then incubated with Alexa Fluor 568–conjugated goat anti-rabbit and 488–conjugated goat anti-mouse antibody and mounted on coverslides for confocal microscopy analysis. (D–F) Untransfected HeLa cells on coverslips were fixed and incubated with affinity-purified polyclonal rabbit anti-EHD1 and mouse anti-MICAL-L1 antibodies and detected using Alexa Fluor 488–conjugated goat anti-rabbit and 568–conjugated goat anti-mouse antibody. Arrows (A–C) depict representative tubules containing both proteins. Insets (D–F) depict higher magnification of the boxed areas. Bar, 10 μm.

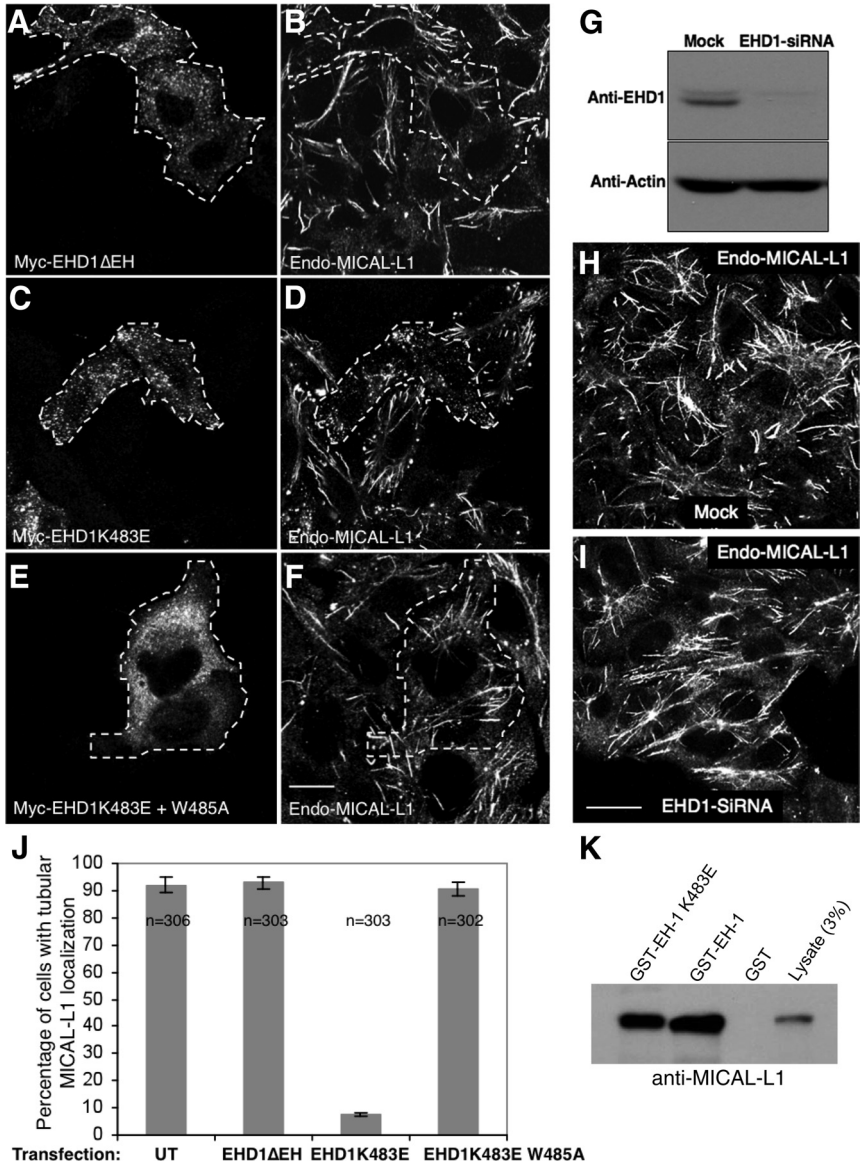

Figure 3. MICAL-L1 associates with tubular membranes independently of EHD1. (A–F) HeLa cells on coverslips were transiently transfected with Myc-EHD1 ΔEH (A and B), Myc-EHD1 K483E (C and D), and Myc-EHD1 K483E+W485A (E and F). After 24 h, cells were fixed and incubated with rabbit anti-Myc antibody and mouse anti-MICAL-L1 antibodies and detected using Alexa Fluor 488–conjugated goat anti-rabbit and Alexa Fluor 568–conjugated goat anti-mouse antibody. Dashed areas indicate transfected cells. (G) HeLa cells growing on 35-mm plates were either mock-treated or treated with EHD1-siRNA and harvested after 72 h. Cells were then lysed and proteins separated by 8% SDS-PAGE before immunoblotting with affinity-purified anti-EHD1 antibodies (top) and monoclonal anti-actin antibody to validate equal protein loading (bottom) followed by anti-rabbit and anti-mouse HRP-conjugated antibodies. ECL was used for detection. (H and I) HeLa cells on coverslips were mock-treated (H) or treated with EHD1-siRNA (I). After 72 h of treatment with siRNA, cells were fixed and stained for endogenous MICAL-L1 followed by 488–conjugated goat anti-mouse secondary antibody. Bar, 10 μm. (J) HeLa cells on coverslips were transfected and processed as described in A–F. Approximately 100 untransfected or cells transfected either with Myc-EHD1 ΔEH, Myc-EHD1 K483E, and Myc-EHD1 K483E+W485A were scored as "containing tubules" or "lacking tubules" from three independent experiments. Error bars, SE. (K) Bacterially expressed, purified recombinant GST, GST-EH-domain of EHD1 (GST-EH-1), or GST-EH domain of EHD1K483E (GST-EH-1 K483E) was incubated with lysates from HeLa cells. The bound proteins were resolved by 8% reducing SDS-PAGE, transferred to nitrocellulose, and immunoblotted with mouse anti-MICAL-L1 to detect binding to endogenous EHD1. After incubation with secondary anti-mouse HRP-conjugated antibodies, ECL was then used for detection.

Association of MICAL-L1 with Tubular Membranes Is Independent of EHD1

To first determine whether EH1-NPF interactions dictate the colocalization between EHD1 and MICAL-L1, we overexpressed Myc-EHD1 lacking its EH domain (Myc-EHD1 ΔEH) and immunostained with antibodies to the Myc-epitope along with endogenous MICAL-L1 (Figure 3, A and B). As demonstrated in the transfected cells (yellow dashed boundaries), and as we have previously described, EHD1 ΔEH (which cannot interact with NPF motifs) localizes to vesicles rather than tubules (Caplan *et al.*, 2002), whereas endogenous MICAL-L1 remains on tubular membranes. To more specifically elucidate the role of EH-domain/NPF interactions, we took advantage of a single amino acid substitution mutant of EHD1 that loses its tubular nature (Naslavsky *et al.*, 2007). As demonstrated in the GST-pull-down assay, despite the loss of association with tubules, the EHD1 K483E mutant still retains its capability of associating with NPF motifs (in this case, endogenous MICAL-L1; Figure 3K). When high levels of the primarily vesicular-localized Myc-EHD1 K483E were overexpressed, the endogenous MICAL-L1 was relocalized to these punctate structures (Figure 3, C and D). As a control, we utilized a double amino acid substitution mutant (Myc-EHD1 K483E + W485A) that is largely vesicular, but can no longer interact with NPF motifs (Naslavsky *et al.*, 2004; Figure 3, E and F). As expected, MICAL-L1 remained primarily tubular (see cells with dashed yellow boundaries), indicating that the EH domain–NPF motif interaction is required for the colocalization of the two proteins. Quantification of the percentage of cells with a tubular MICAL-L1 localization pattern is provided in Figure 3J. These findings suggest that although EHD1 normally does not regulate MICAL-L1 localization to tubules, overexpression of the EHD1 K483E mutant serves as a "dominant-negative," retaining its binding to MICAL-L1, and likely sequestering MICAL-L1 and preventing its own association with the tubules.

Recent studies have provided strong evidence that EHD proteins are ATPases with homology to the dynamin-family of GTPases (Caplan *et al.*, 2002; Lee *et al.*, 2005; Naslavsky *et*

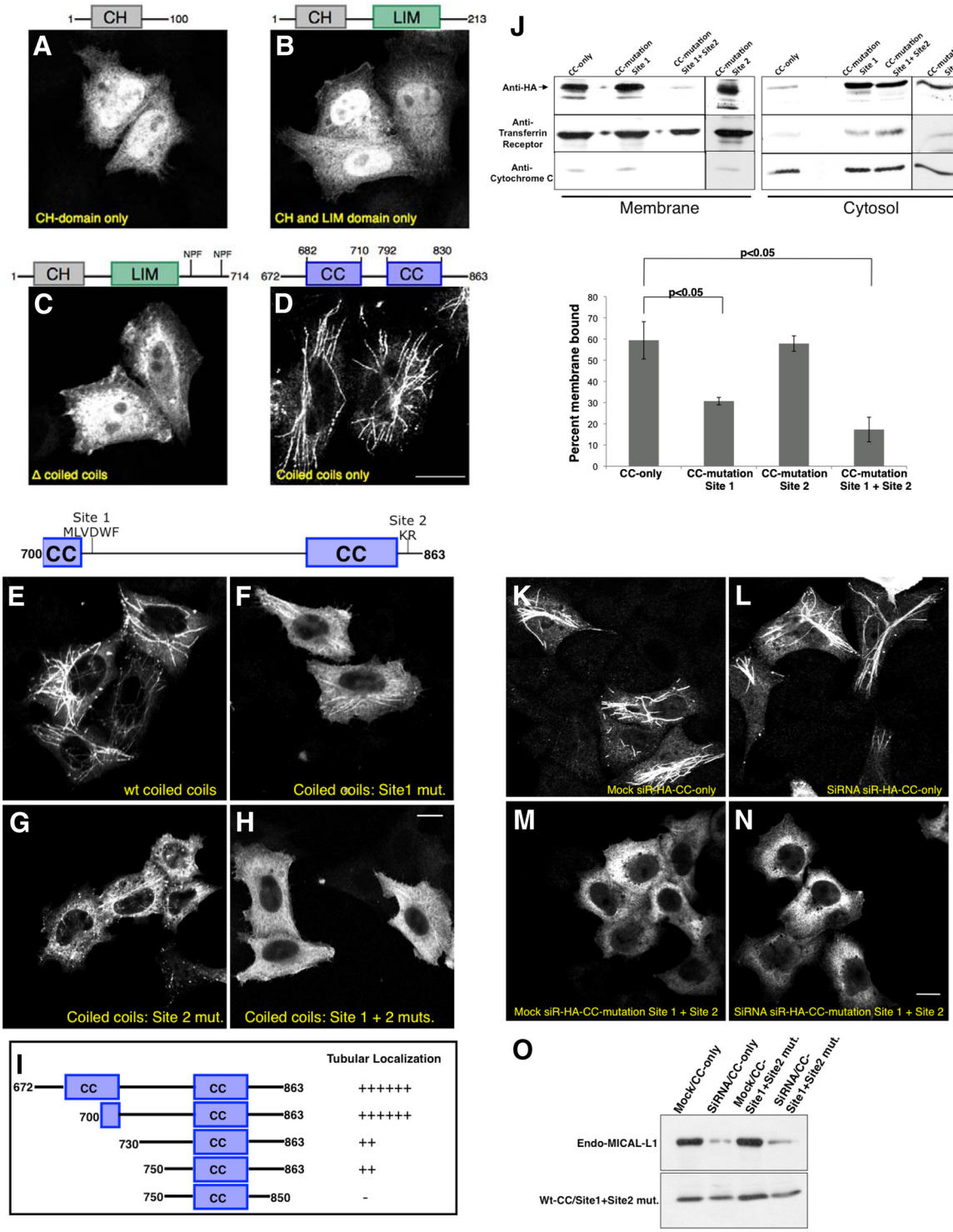

Figure 4. The C-terminal CC region of MICAL-L1 is essential and sufficient for association with tubular membranes. (A–H) HeLa cells on coverslips were transiently transfected with the GFP-MICAL-L1 CH domain only (residues 1–100, A), GFP-MICAL-L1 CH and LIM domains only (residues 1-213, B), GFP-MICAL-L1 Δ CCs (residues 1-714, C), HA-MICAL-L1 CCs only (residues 672-863, D), HA-MICAL-L1 WT CCs (residues 700-863, E), HA-MICAL-L1 CCs: site 1 mutated to alanine residues (F), HA-MICAL-L1 CCs: site 2 mutated to alanine residues (G), HA-MICAL-L1 CCs: site 1 + site 2 mutated to alanine residues (H). After 24 h, cells were fixed and directly analyzed or incubated with mouse anti-HA antibody followed by the appropriate secondary antibodies. (I) HA-MICAL-L1 WT CCs (residues 700–863) was subjected to further deletion/truncation analysis as depicted, expressed in HeLa cells, and analyzed for localization to tubular membranes. (J) HeLa cells growing on 60 mm plates were transiently transfected with either HA-tagged WT CCs (700–863; CC-only), HA-tagged WT CCs with alanine mutations at site 1 (CC-mutation site 1), HA-tagged WT CCs with alanine mutations at site 2 (CC-mutation site 2) or HA-tagged WT CCs with alanine mutations at both sites 1 and 2 (CC-mutation site 1 + site 2). After 48 h, the cells were homogenized in ice-cold homogenization buffer, and postnuclear supernatants were separated to membrane and cytosol fractions by ultracentrifugation. The samples were resolved by 10% SDS-PAGE, transferred to nitrocellulose, and immunoblotted with either anti-HA (top), anti-Tf receptor antibodies (control for membrane

al., 2006; Daumke *et al.*, 2007) and are intrinsically capable of binding negatively charged liposomes in vitro to deform these membranes to produce tubules (Daumke *et al.*, 2007). This suggests that in vivo EHD1 might also generate tubular membranes, and thus MICAL-L1 localization to these tubules should be dependent on EHD1 expression. To test this hypothesis, HeLa cells were either mock-treated or treated with EHD1-siRNA. As depicted, EHD1-siRNA reduced EHD1 expression by ~90% or more in HeLa cells as determined by immunoblot analysis (Figure 3G). Surprisingly, no change in the localization of MICAL-L1 was observed upon EHD1 depletion when compared with mock-treated cells, and endogenous MICAL-L1 continued to associate with tubular membranes (Figure 3, H and I), with 90 and 92% of the cells containing endogenous MICAL-L1 tubules for mock- and EHD1-siRNA–treated cells, respectively.

On the basis of the high level of homology between EHD1 and its paralogs, we tested whether knockdown of EHD pairs might disrupt MICAL-L1 localization to tubules (Supplemental Figure S3). Given that EHD2 displayed no binding to MICAL-L1 (Supplemental Figure S1) and that it displays poor hetero-oligomerization with the other EHDs (Naslavsky *et al.*, 2006; George *et al.*, 2007), we elected to knock down EHD1 together with EHD3 or EHD4. Although the efficiency of depletion is generally decreased when more than one target is knocked down, we were able to establish at least 60–70% reduction of EHD1 when siRNA of EHD1 was used simultaneously with siRNA for EHD3 or EHD4 (Supplemental Figure S3E). At the same time, the level of EHD3 or EHD4 depleted was also between 60 and 80%. However, when we monitored the localization of endogenous MICAL-L1 in hundreds of cells, we found no difference between the double-siRNA–treated and mock-treated cells (Supplemental Figure S3, A–D). Collectively, these results demonstrate that in vivo EHD1 and its paralogs are dispensable for the generation of tubules that normally contain both EHD1 and MICAL-L1.

The C-Terminal CC Region of MICAL-L1 Is Essential and Sufficient for Its Tubular Localization

Recent studies suggest that other MICAL family members such as MICAL-1 and -3 also localize to tubular membranes upon overexpression in HeLa cells (Fischer *et al.*, 2005), despite displaying only 20–30% overall identity with MICAL-L1. Interestingly, these proteins lack the NPF motifs found in MICAL-L1, again suggesting that association with EHD proteins is not required for their tubular localization. We analyzed the roles of different MICAL-L1 domains in mediating binding to the tubular membranes by generating truncation mutants containing one or more isolated domains of MICAL-L1. GFP-tagged deletion mutants of MICAL-L1 containing only the CH domain (Figure 4A), CH and LIM domains (Figure 4B), and the CH and LIM domains along with the NPF motifs (until residue 714; Figure 4C) were unable to associate with membranes and remained largely localized to the cytoplasm. As all these mutants lacked the complete CC region, we hypothesized that it might be responsible for membrane localization. To test this prediction, we next analyzed the localization of the isolated CC region. Surprisingly, this region (residues 672–863) displayed localization to the tubular membranes, clearly indicating that it is both essential and sufficient for the association of MICAL-L1 with these structures (Figure 4D). More extensive deletion analysis of the CC region showed that residues 700–863 frame the minimal region required for tubular localization (Figure 4, E and I). As depicted schematically (Figure 4I), deletion of the region containing residues 700–730 caused a significant decrease in localization to tubules. Moreover, tubule association was further decreased by truncating the last 13 residues (Figure 4I). The region from 700 to 730 was systematically alanine screened by mutating clusters of five amino acids at a time and by testing localization after transfection in HeLa cells (data compiled in Figure 4I). The C-terminal region (750–863) was systematically alanine screened by mutating clusters of three residues at a time. We observed that a stretch of hydrophobic residues beginning at position 721 (MLVDWF site 1) after the first CC is important for membrane association. Replacement of these residues with alanine residues decreased the membrane localization by twofold (Figure 4, F and J). A second site required for optimal membrane association was the positively charged KR duo at position 851-52 (site 2), at the end of the second CC (Figure 4, G and J). Although mutation of the site 2 alone did not significantly impair membrane binding, modification of both of these sites together significantly disrupted the membrane binding of this region of MICAL-L1, rendering it mostly cytosolic (Figure 4, G, H, and J). Consistent with these findings, separation of membrane and cytosolic fractions showed that this region was mostly membrane-bound, with little protein in the cytosol (Figure 4J, top, and quantified in graph). Tf receptor (Figure 4J, middle) and cytochrome C (Figure 4J, bottom) were used as marker proteins for membrane and cytosolic fractions, respectively.

Although the data suggest that the CC region is responsible for the association of MICAL-L1 with tubular membranes, one possibility was that when overexpressed, this CC interacts with the tubular-associated endogenous MICAL-L1. To test this, we used siRNA to deplete endogenous MICAL-L1 and then expressed siRNA-resistant MICAL-L1 CC regions in mock- or siRNA-treated cells (Figure 4O). As demonstrated, endogenous MICAL-L1 depletion was ~90% efficient (Figure 4O, top). On the other hand, expression of the resistant WT and double-mutant (site 1 + site 2 mut.) CCs was similar in mock- and siRNA-treated cells (Figure 4O, bottom). Having effectively introduced the WT and double-mutant MICAL-L1 CCs in cells depleted of endogenous MICAL-L1, we then assessed the ability of the

Figure 4 (cont). fraction, middle) or anti-cytochrome C (control for cytosolic fraction, bottom) followed by anti-mouse HRP-conjugated antibodies. ECL was used for detection. Densitometric analysis was performed on three independent experiments to measure percent membrane-bound. The ratios of membrane-associated to the total protein were then calculated and converted to percentages. Error bars, SE; n = 5 for WT CCs and n = 3 for all three mutants. Significance ($p < 0.05$) was determined by ANOVA. (K–N) HeLa cells on coverslips were mock-treated (K and M) or treated with MICAL-L1-siRNA (L and N). After 48 h, the cells were transfected with siRNA-resistant HA-tagged WT CCs (700–863, siR-HA-CC-only, K and L) or with siRNA-resistant HA-tagged WT CCs with alanine mutations at both sites 1 and 2 (siR-HA-CC-mutation site 1 + 2, M and N). After an additional 24 h, the cells were fixed and incubated with mouse anti-HA antibodies followed by staining with Alexa Fluor 488–conjugated goat anti-mouse antibody. (O) HeLa cells growing on 35-mm plates were either mock-treated or treated with MICAL-L1-siRNA. After 48 h, the cells were transfected with siR-HA-CC-only or with siR-HA-CC-mutation site 1 + 2. After an additional 24 h, the cells were lysed and proteins separated by 8% SDS-PAGE were subjected to immunoblotting with anti-MICAL-L1 antibodies (top) and monoclonal anti-HA antibody to verify expression of the transfected constructs (bottom), followed by anti-mouse HRP-conjugated antibodies. ECL was used for detection. Bar, 10 μm.

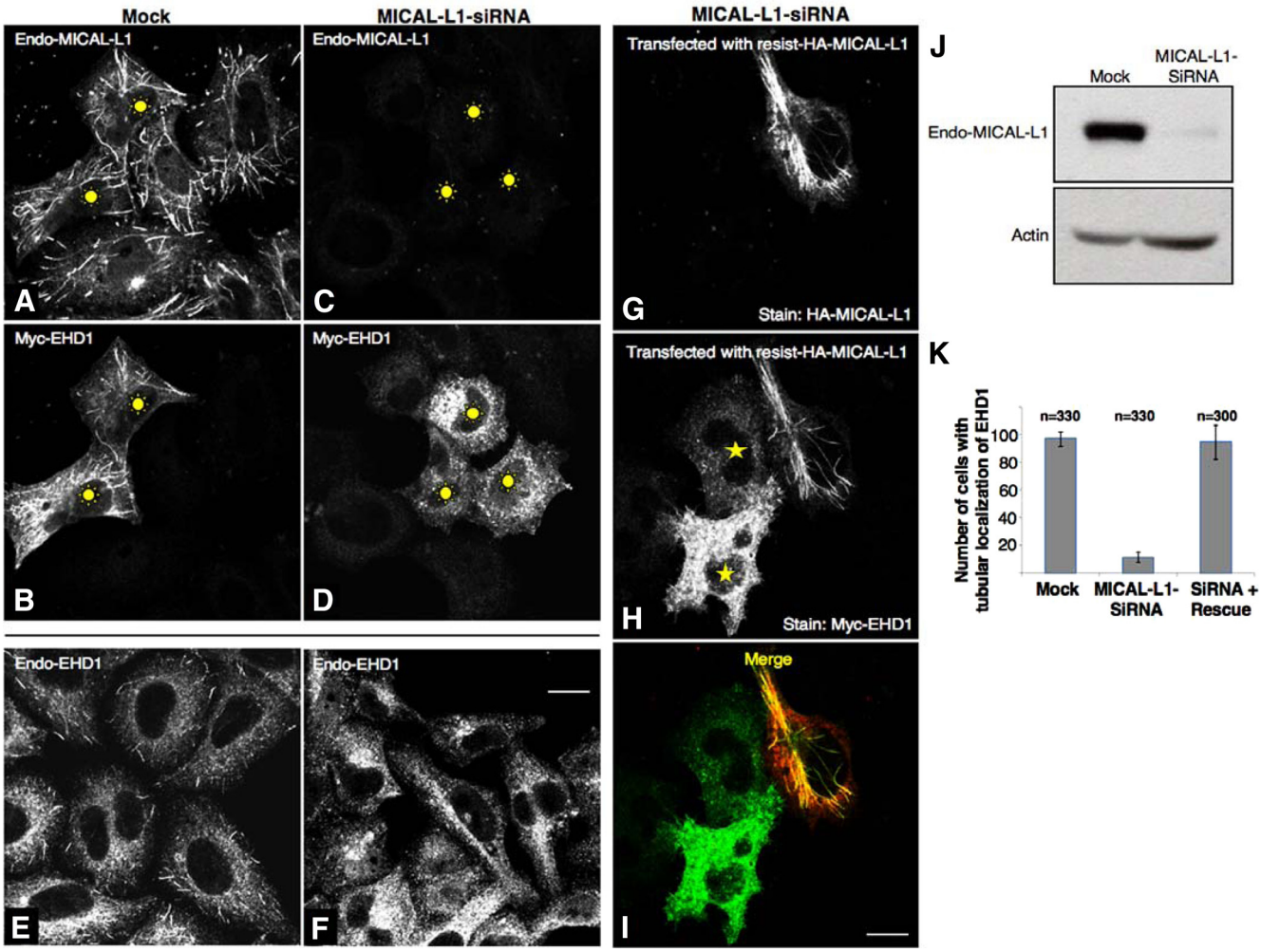

Figure 5. MICAL-L1 is required for the association of EHD1 with tubular membranes. (A–D) HeLa cells on coverslips were mock-treated (A and B) or treated with MICAL-L1-siRNA (C and D). After 48 h, the cells were transfected with Myc-EHD1 (B and D). After an additional 24 h, the cells were fixed and incubated with rabbit anti-Myc antibody and mouse anti-MICAL-L1 antibodies followed by staining with Alexa Fluor 488–conjugated goat anti-rabbit and Alexa Fluor 568–conjugated goat anti-mouse antibody. (E and F) HeLa cells on coverslips were mock-treated (E) or treated with MICAL-L1-siRNA (F). Seventy-two hours later the cells were fixed and stained for endogenous EHD1 (E and F) followed by Alexa Fluor 568–conjugated goat anti-rabbit antibody. (G–I) MICAL-L1-siRNA-treated cells were cotransfected with an siRNA-resistant HA-MICAL-L1 construct and Myc-EHD1. Cells were fixed, permeabilized, and immunostained with anti-HA (G and I) and anti-Myc (H and I) followed by the appropriate secondary antibodies. Bar, 10 μm. (J) HeLa cells growing on 35-mm plates were either mock-treated or treated with MICAL-L1-siRNA and harvested after 72 h. Cells were then lysed, and proteins separated by 8% SDS-PAGE were subjected to immunoblotting with anti-MICAL-L1 antibodies (top) and monoclonal anti-actin antibody to validate equal protein loading (bottom), followed by anti-mouse HRP-conjugated antibodies. ECL was used for detection. (K) HeLa cells on coverslips were either mock-treated or treated with MICAL-L1-siRNA. After 48 h, the cells were either transfected with only Myc-EHD1 (mock and MICAL-L1-siRNA) or cotransfected with both Myc-EHD1 and siRNA-resistant HA-MICAL-L1 (siRNA + Rescue) and stained as described above. Approximately 100 cells transfected with Myc-EHD1 from three independent experiments were counted for each set of treatments. Error bars, SE. Sunbursts denote Myc-EHD1-transfected cells (A–D), stars denote cells transfected with Myc-EHD1, but not HA-MICAL-L1 (H).

CC domains to associate with tubular membranes (Figure 4, K–N). As demonstrated, in either mock- or siRNA-treated cells, the WT CCs localized to tubular membranes (Figure 4, K and L), suggesting that this region is capable on its own of associating with tubular membranes. Further support for this notion comes from our finding that MICAL-L1 displays poor homo-oligomerization (Supplemental Figure S1A). However, CCs with modifications in the hydrophobic patch and KR residues remained dissociated from the tubular membranes (Figure 4, M and N). These data are consistent with the MICAL-L1 CC being required and sufficient for association with tubular membranes.

MICAL-L1 Is Required for the Association of EHD1 with Tubular Membranes

Given that the association of MICAL-L1 with tubules is independent of EHD1 expression, we next sought to establish whether MICAL-L1 expression is required for the association of EHD1 with these tubular membranes. To this aim, we used siRNA-based knockdown to reduce MICAL-L1 expression in HeLa cells (Figure 5J, top). To test the effect of MICAL-L1 depletion on EHD1 localization, both mock- and MICAL-L1-siRNA–treated cells were transfected with Myc-EHD1. As shown, endogenous MICAL-L1 staining was

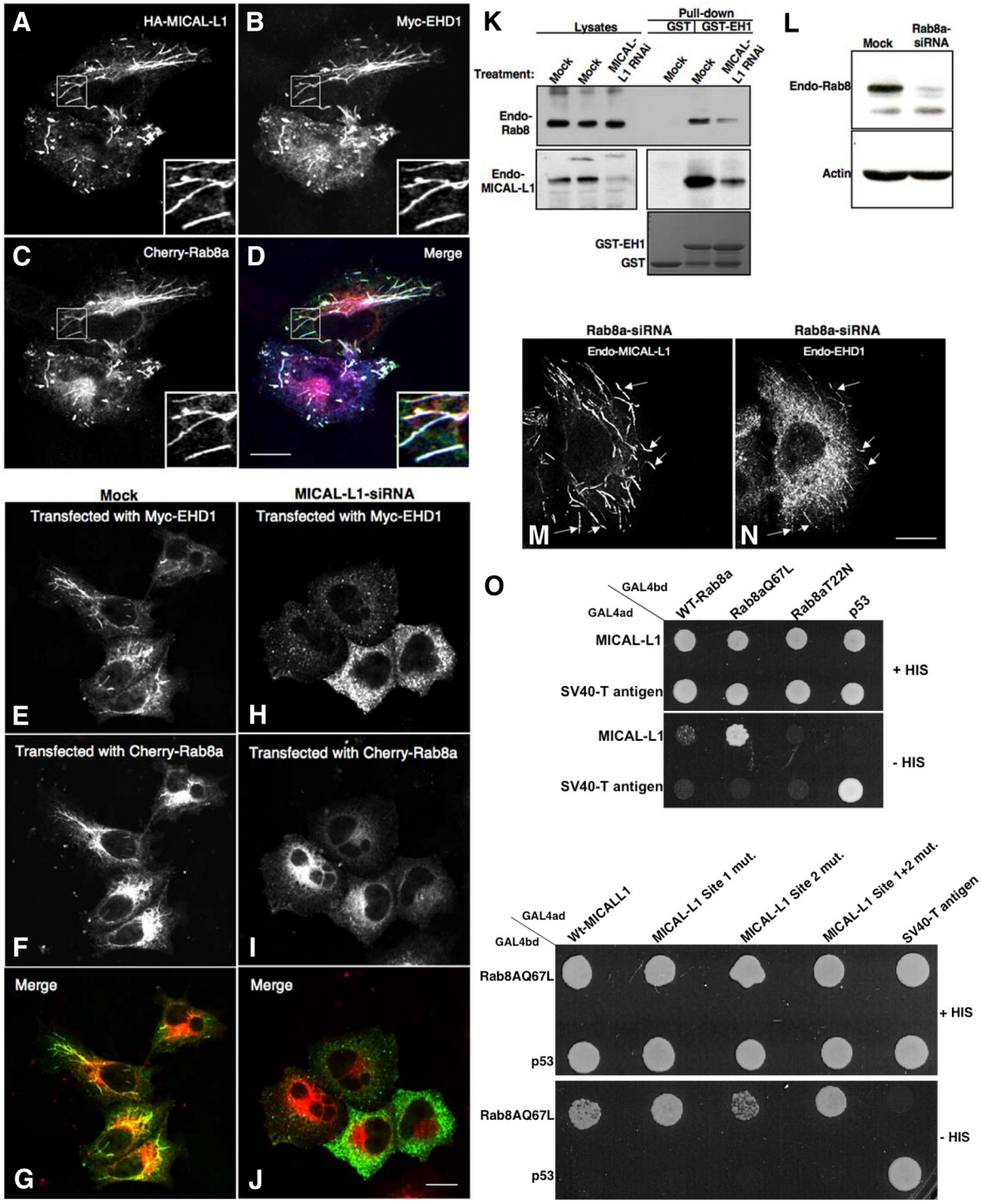

Figure 6. MICAL-L1 is responsible for the colocalization and coassociation of Rab8a and EHD1 on tubular membranes. (A–D) HeLa cells on coverslips were transiently triple-transfected with HA-MICAL-L1 (A and D), Myc-EHD1 (B and D), and Cherry-Rab8a (C and D). After 24 h, cells were fixed and incubated with rabbit anti-Myc antibody and mouse anti-HA antibody. The cells were then incubated with Alexa Fluor 405–conjugated goat anti-rabbit and Alexa Fluor 488–conjugated goat anti-mouse antibody and mounted on coverslides. Bar, 10 μm. (E–J) HeLa cells on coverslips were mock-treated (E–G) or treated with MICAL-L1-siRNA (H–J). After 48 h, the cells were cotransfected with Myc-EHD1 and Cherry-Rab8a. Twenty-four hours later the cells were fixed and incubated with rabbit anti-Myc antibody followed by staining with Alexa Fluor 488–conjugated goat anti-rabbit antibody. (K) Bacterially expressed, recombinant GST or GST fused to the EH domain of EHD1 (GST-EH1) was incubated with lysates from HeLa cells either mock-treated or treated with MICAL-L1-siRNA. The bound proteins were resolved by 8% SDS-PAGE, transferred to nitrocellulose, and immunoblotted with mouse anti-Rab8a (top) followed by anti-mouse HRP-conjugated antibodies. The same blot was stripped with 3 M guanidinium isothiocyanate and probed with mouse anti-MICAL-L1 antibody (middle). ECL was used for detection. GST- and GST-EH1–purified protein bands shown in bottom panel were visualized with Coomassie blue dye staining. (L) HeLa cells growing on 35-mm plates were either mock-treated or treated with Rab8a-siRNA and harvested after 72 h. Cells were then lysed, and proteins were separated by 10% SDS-PAGE and subjected to immunoblotting with anti-Rab8a

practically absent in MICAL-L1-siRNA–treated cells compared with mock-treated cells (cf. Figure 5, A and C). Surprisingly, we found that there was a very dramatic loss of EHD1 association with tubular membranes in cells lacking MICAL-L1, with only vesicular staining of EHD1 in evidence (cf. Figure 5, B and D). Moreover, the tubular localization of endogenous EHD1 was also disrupted upon loss of MICAL-L1 (Figure 5, E and F), indicating that under physiological conditions as well, MICAL-L1 is essential for the association of EHD1 with tubular membranes.

We also tested whether MICAL-L1 expression affected the distribution of the other EHD proteins. As demonstrated in Supplemental Figure S4, depletion of endogenous MICAL-L1 had a modest effect on EHD3, partially displacing it from tubular membranes, but not to the same degree as it affected EHD1 (Supplemental Figure S4; cf. A–C with D–F). EHD4, which hetero-oligomerizes with EHD1 and requires EHD1 expression for its own partial localization to tubular membranes (Sharma *et al.*, 2008), showed a more dramatic dissociation from tubules upon MICAL-L1-depletion (Supplemental Figure S4; cf. G–I with J–L). However, EHD2, which does not interact with MICAL-L1 or the other EHDs, did not display any loss of tubule association in the absence of MICAL-L1 (Supplemental Figure S6A and B).

To provide additional evidence that MICAL-L1 depletion is specifically responsible for the loss of EHD1 from tubular membranes, we utilized a siRNA-resistant MICAL-L1 construct engineered with silent mutations in the region recognized by the oligonucleotides. To this end, we expressed MICAL-L1 siRNA-resistant silent HA–MICAL-L1 in cells treated with MICAL-L1-siRNA. As shown (Figure 5, G–I), the silent HA-MICAL-L1 "rescued" the effect of the siRNA knockdown, resulting in EHD1 associating with tubular membranes. However, in the siRNA-treated, but nontransfected cells, EHD1 was unable to associate with tubules (Figure 5H, compare the two marked cells with the unmarked cell). To quantitatively evaluate the degree to which localization of EHD1 to tubules relies on MICAL-L1 expression and to determine if siRNA-resistant MICAL-L1 can rescue the effect of MICAL-L1 knockdown, we treated cells with either mock- or MICAL-L1-siRNA and transfected with either Myc-EHD1 alone, or cotransfected Myc-EHD1 together with the silent MICAL-L1 as described above. On MICAL-L1-depletion, we observed EHD1 localized to tubules in <10% of the cells (a ninefold difference; Figure 5K). However, this effect was rescued by the expression of siRNA-resistant MICAL-L1 (Figure 5K). These data strongly suggest that MICAL-L1 is responsible for the association of EHD1 with tubular membranes, and that MICAL-L1 may have a direct bearing on the regulatory function of EHD1 in endocytic recycling.

Figure 6 (cont). antibodies (top) and monoclonal anti-actin antibody to validate equal protein loading (bottom) followed by anti-mouse HRP-conjugated antibodies. ECL was used for detection. (M and N) HeLa cells on coverslips were treated with Rab8a-siRNA. After 72 h, the cells were fixed and stained for endogenous MICAL-L1 (M) and endogenous EHD1 (N) followed by the appropriate secondary antibodies. Arrows denote colocalization on tubules. Bars, 10 μm. (O) The *S. cerevisiae* yeast strain AH109 was cotransformed with the indicated GAL4-binding domain (GAL4bd) fusion constructs and Galbd-p53 (control), together with the indicated GAL4 transcription activation (GAL4ad) fusion constructs and GAL4ad-SV40 large T-antigen (control). Cotransformants were assayed for their growth on nonselective (+HIS) and selective (−HIS) media.

MICAL-L1 Links EHD1 with Rab8a and Is Responsible for Their Coassociation on the Tubular Membranes

Endogenous Rab8a is localized to tubular and vesicular membranes that extensively colocalize with the EHD1 tubular compartment (Roland *et al.*, 2007). Rab8a also regulates the recycling of Tf receptors and localizes to tubules containing β1 integrins (Hattula *et al.*, 2006). As both Tf and β1 integrin receptors recycle in an EHD1-dependent manner (Lin *et al.*, 2001; Naslavsky *et al.*, 2004; Jovic *et al.*, 2007), this suggests functional coordination between EHD1 and Rab8a in regulating endocytic recycling events. However, the mode by which Rab8a is recruited to and linked with the EHD1-tubular network and how these two proteins coordinately regulate receptor recycling is unknown to date. Our recent study shows that EHD1 depletion has no affect on Rab8a localization to tubules suggesting that Rab8a is not recruited to the tubules via a direct interaction with EHD1. On the other hand, MICAL-L1 directly binds to GTP-bound Rab8a via its C-terminal CC domains (Fukuda *et al.*, 2008; Yamamura *et al.*, 2008). On the basis of these observations, we hypothesized that MICAL-L1 might be the critical link between EHD1 and Rab8a and may be involved in their recruitment to tubular membranes, enabling them to regulate recycling of various receptors.

To test this hypothesis, we simultaneously overexpressed Cherry-Rab8a, Myc-EHD1, and HA-MICAL-L1 and found very high levels of colocalization for all three proteins on the tubular membranes (Figure 6, A–D). To directly test the role of MICAL-L1 in colocalization and coassociation of EHD1 and Rab8a, we depleted MICAL-L1 using siRNA and analyzed the localization of EHD1 with Rab8a. Partial but significant colocalization of EHD1 and Rab8a on the tubular endosomes was observed in the mock-treated cells (Figure 6, E–G). Interestingly, upon MICAL-L1-depletion, both EHD1 and Rab8a underwent dissociation from the tubular endosomes. In MICAL-L1-siRNA–treated cells, EHD1 localized exclusively to vesicular (and nontubular) membranes, some of which contain the early endosomal marker, EEA1 (Supplemental Figure S5, A–F), whereas Rab8a localized primarily to the ERC (and partially overlapped with Tf receptor; see Supplemental Figure S5, G–L), with little colocalization remaining between EHD1 and Rab8a (Figure 6, H–J).

As noted earlier, no effect of MICAL-L1 depletion was observed on the localization of EHD2 (Supplemental Figure S6, A and B), endogenous Rab11 (Supplemental Figure S6, C and D), or GFP fused to the double palmitoylated and farnesylated carboxyl terminal tail of H-Ras (H-Ras; Supplemental Figure S6, E and F), all of which normally display partial colocalization with EHD1-containing tubular membranes at the ERC. Indeed, upon triple staining (Supplemental Figure S6, G and H), we observed a high level of colocalization between EHD1, MICAL-L1, and H-Ras, suggesting that both EHD1 and MICAL-L1 decorate existing tubular membranes. Overall, these data imply that loss of MICAL-L1 specifically affects its in vivo interaction partners, EHD1 and Rab8a.

To further confirm our studies indicating that MICAL-L1 serves as a nexus to link EHD1 and Rab8a on membrane tubules, we performed pulldown assays using the GST-EH1 from both mock- and MICAL-L1-siRNA–treated cells. Endogenous Rab8a and endogenous MICAL-L1 were both pulled down by the GST-EH1; however, there was a significant loss of binding of Rab8a with the GST-EH1 in lysates from MICAL-L1–depleted cells (Figure 6K), reinforcing our conclusion that MICAL-L1 is the critical link by which these two endocytic proteins are recruited to the tubular recycling

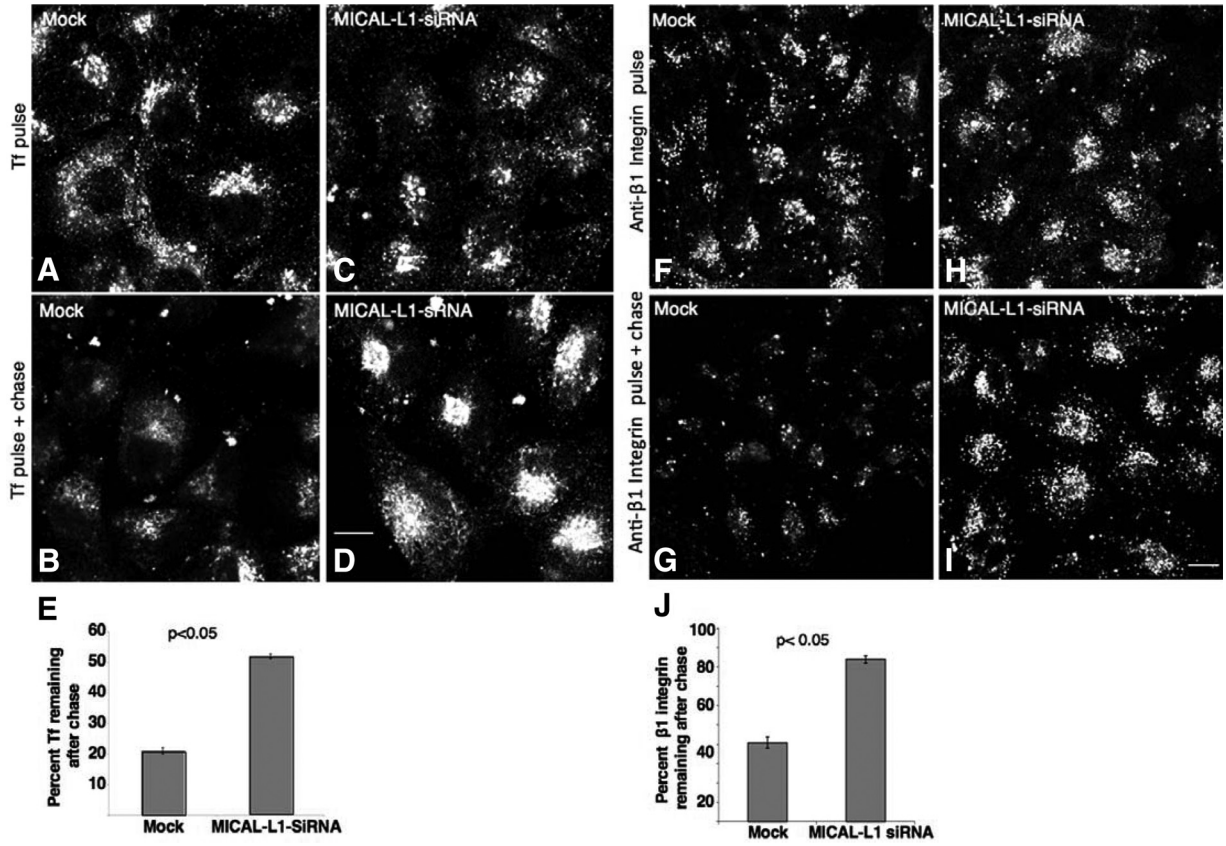

Figure 7. MICAL-L1 regulates the recycling of Tf receptor and β1 integrins back to the plasma membrane. (A–D) HeLa cells on coverslips were mock-treated (A and B) or treated with MICAL-L1-siRNA (C and D). Seventy-two hours later the cells were serum-starved for 30 min and pulsed with Tf-568 for 10 min and fixed (A and C), or first "chased" in complete medium for 25 min at 37°C before fixation (B and D). (E) Quantitative analysis of the percentage of internalized Tf remaining after 15 min of pulse and 40 min of chase was done. Approximately 80 cells from three independent experiments were counted for each set of treatments. Error bars, SE. (F–I) HeLa cells on coverslips were mock-treated (F and G) or treated with MICAL-L1-siRNA (H and I) for 72 h. Cells were then starved and pulsed with anti-β1 integrin antibody for 1 h and fixed (F and H) or pulsed for 1 h and chased in complete media for 3 additional hours at 37°C before fixation (G and I). (J) Quantitative analysis of the percentage of β1 integrins remaining after 3 h of chase was done as described for Tf. Significance ($p < 0.05$) was determined by the Student's *t* test for independent samples. Bar, 10 μm.

compartment. The residual and weak binding of Rab8a with the EH1 in the MICAL-L1-siRNA–treated cell lysate may be attributed to incomplete knockdown of MICAL-L1. As shown, low levels of MICAL-L1 were still present in siRNA-treated cell lysates pulled down with GST-EH domain (Figure 6K, bottom panel). Because the CC region of MICAL-L1 is required both for association with Rab8a (Fukuda *et al.*, 2008; Yamamura *et al.*, 2008) and for association with tubular membranes, we wanted to test whether Rab8a expression might regulate the localization of MICAL-L1, and thus EHD1, on the tubular membranes. Using siRNA specific for Rab8a, we could achieve ~80–90% knockdown of Rab8a (Figure 6L). Interestingly, we did not observe any change in localization of EHD1 or MICAL-L1 upon Rab8a knockdown, with both proteins continuing to colocalize on the tubular endosomes (Figure 6, M and N). Moreover, as demonstrated in Figure 6O, although MICAL-L1 binds almost exclusively to the GTP-locked Rab8aQ67L mutant, the MICAL-L1 CC mutants (including the double mutant), despite losing their ability to associate with membranes, were nonetheless still capable of associating with active Rab8a, further suggesting that MICAL-L1 binds to tubular membranes independently of Rab8a. Furthermore, expression of the MICAL-L1 CC region significantly stabilized Rab8a on the tubular membranes (see Supplemental Figure S7, A–G). Accordingly, on the basis of these findings we propose a model whereby MICAL-L1 is first recruited to the tubular recycling compartment, independently of EHD1 or Rab8a expression, and is necessary for the recruitment of both EHD1 and Rab8a to these tubules by potentially binding them through distinct domains.

MICAL-L1 Is a Novel Regulator of Endocytic Recycling from the ERC to the Plasma Membrane

Finally, on the basis of our observations that MICAL-L1 is essential for the tubular membrane localization of EHD1, which mediates the endocytic recycling of various receptors, we hypothesized that MICAL-L1 is a novel regulator of the "slow recycling" pathway. To address this, we treated cells with MICAL-L1-siRNA and monitored the trafficking of Tf and β1 integrin receptors. HeLa cells on coverslips were either mock-treated (Figure 7, A and B) or treated with MICAL-L1-siRNA (Figure 7, C and D) and subjected to "pulse-chase" experiments with fluorochrome-labeled Tf (Tf-568). After the pulse with Tf-568, both mock- and MICAL-L1-siRNA–treated cells exhibited a similar subcellular distribution of internalized Tf-568 (Figure 7, A and C). However, after a 25-min chase, mock-treated cells had recycled most of their internalized Tf-568 to the plasma membrane, whereas MICAL-L1–depleted cells exhibited significant ac-

cumulation of Tf in the ERC (Figure 7, B and D). Quantification of three independent experiments demonstrated that MICAL-L1-siRNA–treated cells retained 50% of the internalized Tf-568 compared with only 20% remaining in the mock-treated cells (Figure 7E). In addition, we monitored the recycling of internalized Tf-568 in cells transfected with GFP-MICAL-L1 in live cells by time-lapse microscopy (see Supplemental Figure S8). As expected, much of the MICAL-L1 was localized to tubular membrane structures that primarily emanated from the perinuclear recycling compartment. Although the internalized Tf first accumulated in this region and then emptied from this compartment as recycling occurred over time, surprisingly, a significant level of Tf could be detected aligning along tubular membranes decorated by MICAL-L1 (Supplemental Figure S8; see yellow arrows and inset). Indeed, even in untransfected cells, internalized Tf could occasionally be observed on tubular membranes; however, such tubular localization of Tf is rarely observed in fixed cells.

We also analyzed the recycling of cargo internalized via clathrin-independent pathways, such as the β1 integrin receptor upon MICAL-L1 depletion. Although internalized levels of β1 integrins were similar in mock-treated and MICAL-L1–depleted cells (Figure 7, F and H), most of the internalized β1 integrins failed to recycle efficiently in knockdown cells compared with the mock-treated cells (cf. Figure 7, G and I). Quantification of three independent experiments demonstrated a significant delay in β1 integrin recycling upon MICAL-L1 knockdown, with 84% of the internalized β1 integrin receptors still remaining in the siRNAi-treated cells compared with 40% remaining in the mock-treated cells (Figure 7J). Although Rab8a clearly has additional roles to those proposed in recycling (Huber *et al.*, 1993; Ang *et al.*, 2003; Hattula *et al.*, 2006; Linder *et al.*, 2006; Roland *et al.*, 2007; Henry and Sheff, 2008), we reasoned that because it is linked to MICAL-L1 and EHD1, it may partially contribute to the regulation of β1 integrin recycling. To avoid potential compensation from Rab8b, we used siRNA to deplete both Rab8a and Rab8b simultaneously and assayed the effect of this depletion on β1 integrin recycling (see Supplemental Figure S9). As demonstrated, although the knockdown did not delay recycling as dramatically as MICAL-L1, there was a modest but consistent delay in the return of β1 integrins to the plasma membrane. Taken together these results implicate for the first time MICAL-L1 in regulating receptor recycling from ERC back to the plasma membrane and indicate that this regulation occurs through EHD1 and potentially via Rab8.

DISCUSSION

MICAL-L1 Is Essential for the Association of EHD1 with Tubular Recycling Endosomes

Recent studies have contributed to our understanding of the molecular mechanisms by which C-terminal EHD proteins regulate endocytic trafficking events (reviewed in Grant and Caplan, 2008). We have demonstrated that EHD1-containing tubular membranes are required for efficient recycling of Tf and β1 integrin receptors, as the impaired receptor recycling typically observed upon EHD1 depletion is not rescued upon introduction of a nontubular EHD1 mutant protein (Jovic *et al.*, 2009). *How* the EHD1-containing tubules facilitate recycling remains an open question. One possibility is that the localization of EHD1 to the tubules provides a "platform" for the association of motor proteins that might drive recycling vesicles from the ERC to the plasma membrane. For example, myosin Vb interacts with Rab8a on EHD-containing tubules and could serve such a function (Roland *et al.*, 2007). A second possibility (that is not mutually exclusive from the former one) is that EHD1, having intrinsic ATPase activity, acts as a "pinchase" to promote budding of vesicles from tubules that emanate from the ERC, thus facilitating vesicular transport to the plasma membrane (Sharma *et al.*, 2009).

A second key question is whether EHD1 initiates tubule biogenesis or whether it localizes to an existing network of tubules within the cell. Although the recent crystal structure of the mouse EHD2 protein and in vitro lipid-deforming assays clearly demonstrate that EHD proteins can tubulate membranes into ~20-nm diameter tubules (Daumke *et al.*, 2007), our recent studies suggest that the situation in vivo, where we observe tubules of up to 200 nm in diameter, may be more complex (Jovic *et al.*, 2009). For example, Rab8a displays a partial colocalization with EHD1 on tubular membranes, and its association with these structures is retained even upon EHD1 depletion (Jovic *et al.*, 2009). Moreover, we now demonstrate that endogenous MICAL-L1 and EHD1 show an almost complete colocalization to the same tubular membranes, and MICAL-L1 continues to localize to these structures even in the absence of EHD1 expression. These data unequivocally support the notion that in vivo, EHD1 is recruited to preexisting tubular membranes and is not required to induce membrane tubulation.

MICAL-L1 is a member of the MICAL family of proteins, originally described as interaction partners of the focal adhesion plaque protein CasL/HEF1/NEDD9 (Suzuki *et al.*, 2002). Family members display broad homology and generally have both CH and LIM domains. Additionally, several MICAL-family proteins have flavin-adenine dinucleotide (FAD)-binding domains and CC regions (reviewed in Nishimura and Sasaki, 2008). Although MICAL proteins have been proposed to link Rab proteins to the cytoskeleton (Fischer *et al.*, 2005; Nishimura and Sasaki, 2008; Yamamura *et al.*, 2008), their diverse roles in the cell are only beginning to be divulged (reviewed in Fischer *et al.*, 2005; Nishimura and Sasaki, 2008). Of the MICAL-family proteins, MICAL-L1 has not been well characterized and is unique for several reasons: first, its closest homolog, MICAL-L2, displays only ~30% identity. Second, MICAL-L2, which has been implicated in the regulation of cell junctions and in controlling the recycling of the protein occludin to tight junctions, has been localized to the plasma membrane (Terai *et al.*, 2006), whereas we have observed MICAL-L1 distinctly on tubular endosomes that correlate with the ERC. Third, it contains two NPF motifs, and we have provided compelling evidence that the first of these two motifs is necessary for the MICAL-L1–EHD1 interaction. It has been suggested that MICAL-L1 may play a minor role in regulating transepithelial electrical resistance at tight junctions similar to MICAL-L2 (Yamamura *et al.*, 2008), but until now the functional role of MICAL-L1 has remained enigmatic.

Endogenous MICAL-L1 localizes to tubular membranes that overlap almost completely with those containing endogenous EHD1. Given that MICAL-L1 interacts with EHD1 through its first NPF motif, and EHDs were proposed to possess membrane remodeling activity (Daumke *et al.*, 2007), it was reasonable to hypothesize that EHD1 recruits MICAL-L1 to these structures. Surprisingly, several lines of evidence support the idea that MICAL-L1 associates with tubular membranes independently of EHD1. For example, upon depletion of EHD1 from cells, endogenous and overexpressed MICAL-L1 remained highly localized to tubular membranes. In addition, through mapping experiments we

have determined that a region at the C-terminal end of MICAL-L1 that includes the CCs, but *not* the NPF motifs, is required and sufficient for tubular membrane association. In support of this notion, MICAL-1, which also contains a CC region, has also been localized to tubular membranes in HeLa cells (Fischer *et al.*, 2005).

MICAL-L1 Recruits EHD1 to Tubular Membranes and Is Required for Endocytic Recycling

As one of the functions of MICAL proteins is their binding to Rab proteins (Weide *et al.*, 2003; Fukuda *et al.*, 2008), similar to most Rab effector proteins, the interactions between MICAL-family proteins and Rab proteins are generally enhanced when the Rabs are in their GTP-bound state (Weide *et al.*, 2003; Fischer *et al.*, 2005; Fukuda *et al.*, 2008; Yamamura *et al.*, 2008). Our own coimmunoprecipitation and pulldown assays with Rab8a were especially sensitive to the Rab8a nucleotide status, and if GTPγS was omitted from either precipitations or even subsequent washes, the level of Rab8a-MICAL-L1 interaction was dramatically reduced. On the other hand, MICAL-L1 does not behave like most Rab effectors, as our data demonstrate that this protein is recruited independently of Rab8a to the tubular membranes. Indeed, MICAL-L1 depletion also leads to the loss of EHD1 from these structures. Although EHD1 and Rab8a do not interact directly and MICAL-L1 may complex individually with EHD1 and Rab8a, these findings hint that MICAL-L1 may play a role in bridging Rab8a and EHD1 on the tubular endosomes that are required for efficient recycling (see model in Figure 8). Further support for this notion is derived from our findings that depletion of MICAL-L1 impairs the recycling of Tf receptors and β1 integrin receptors, which are internalized through clathrin-dependent and -independent pathways, respectively. Indeed, by our hands depletion of Rab8a/Rab8b leads to a modest reduction in the rate of β1 integrin recycling, consistent with published studies (Hattula *et al.*, 2006; Roland *et al.*, 2007). However, because Rab8a clearly plays additional roles aside from its proposed regulation of recycling (Huber *et al.*, 1993; Ang *et al.*, 2003; Henry and Sheff, 2008), it may act independently of MICAL-L1 and EHD1.

In conclusion, we have identified MICAL-L1 as an EHD1-binding protein that may link EHD1 and Rab8a on tubular recycling endosomes. MICAL-L1 may be capable of interacting directly with phosphoinositides, a characteristic that is common to some Rab effectors. For example, the divalent Rab4/5 effector Rabenosyn-5, directly binds to phosphatidylinositol-3-phosphate through its FYVE domain, while interacting with EHD1 through several of its NPF motifs (Naslavsky *et al.*, 2004). Indeed, through additional alanine screening we have identified two motifs within the CC region that may facilitate association with membranes. The first site contains a hydrophobic stretch potentially compatible with membrane binding, whereas the second site contains a pair of positively charged residues that might allow interaction with phosphoinositides. Ultimately, structural analysis will be needed to conclusively dissect the mode of membrane association. However, unlike Rabenosyn-5 and other Rab effectors that interact with EHD1, such as Rab11-FIP2 (Naslavsky *et al.*, 2004, 2006), MICAL-L1 is necessary for the localization of EHD1 (and Rab8a) to tubular membranes. Although it remains possible that the MICAL-L1 localization to tubules may be regulated by Rab10 or Rab13, two Rabs that directly bind to MICAL family proteins (Fischer *et al.*, 2005; Nishimura and Sasaki, 2008; Yamamura *et al.*, 2008), Rab8a is clearly dispensable for the localization of MICAL-L1 and is itself controlled by MICAL-L1 expression. Although we cannot rule out the possibility that MICAL-L1 induces tubule formation, the lack of homology to a BAR (Bin/Amphiphysin/Rvs) domain and the absence of either an ATP- or a GTP-binding motif supports the likelihood that MICAL-L1 also binds to preexisting tubular membranes. Indeed, it is likely that MICAL-L1 first associates with the tubular membranes and then either recruits EHD1 or stabilizes EHD1 on these structures once they have come into contact. Although the protein(s) that is required for the biogenesis of MICAL-L1/EHD1/Rab8a-containing tubular membranes has not been identified, potential candidates are the BAR domain–containing proteins Syndapin I and II, both of which contain NPF motifs and interact with EHD1 (Xu *et al.*, 2004; Braun *et al.*, 2005). Nonetheless, it is clear that

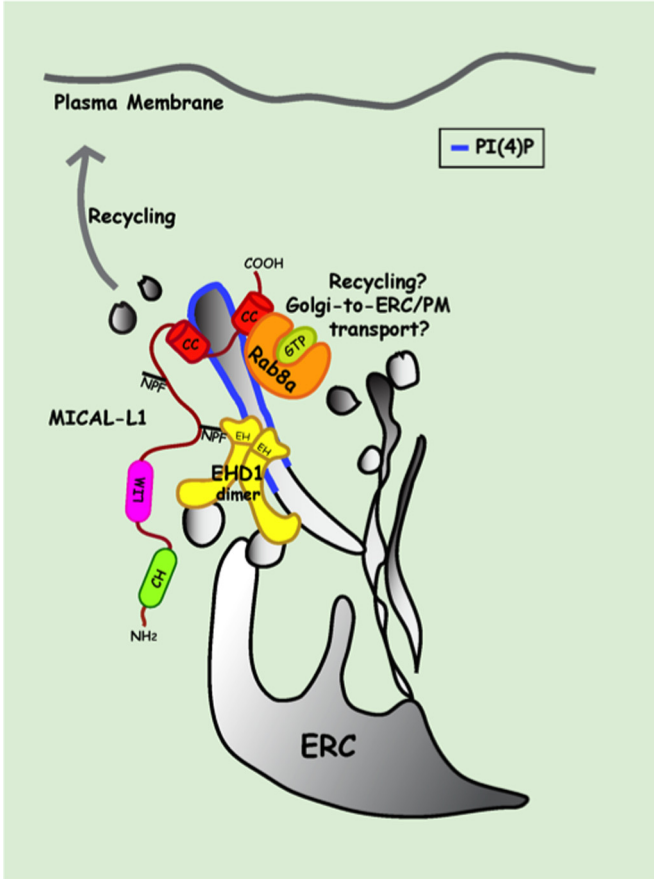

Figure 8. Potential model depicting MICAL-L1 interactions with EHD1 and Rab8a on tubular recycling endosome membranes. MICAL-L1 is recruited to the membranes of tubular recycling endosomes (blue bars) by its C-terminal CC region. Through the binding of its first NPF motif with the EHD1 EH domain (EH1), it recruits and/or stabilizes EHD1 on these tubules. EHD1 is further stabilized on these membranes by the ability of EH1 to directly bind phosphoinositides, specifically PI4P. MICAL-L1 also directly binds to GTP-bound Rab8a and recruits/and or stabilizes it on the tubular membranes; such binding might be simultaneous or independent of EHD1. Localization of EHD1 to the tubular recycling compartment facilitates receptor recycling from the ERC back to the plasma membrane. Rab8a localization to tubular membranes may also play a minor role in EHD1 and MICAL-L1–mediated endocytic recycling pathway. However, as both EHD1 and Rab8a have been implicated in trafficking from the Golgi compartment, their association through MICAL-L1 might be important for trafficking of cargo from Golgi to the plasma membrane or Golgi-to-ERC transport. ERC, endocytic recycling compartment; PI4P, phosphotidylinositol-4-phosphate.

the association of MICAL-L1 with membranes and its ability to recruit or stabilize EHD1 (and potentially Rab8a) on tubular endosomes is essential for efficient endocytic recycling to the plasma membrane.

ACKNOWLEDGMENTS

We thank Drs. J. Donaldson and J. Goldenring for generously providing reagents and are grateful to Dr. R. MacDonald and members of the laboratory for their critical readings. We also thank Dr. Peter Backlund, Jr. (NIH) and the UNMC Mass Spectrometry Core Facility for their assistance. This work was supported by a Grant GM074876 from the National Institutes of Health (S.C.) and an American Heart Association student fellowship (M.S.).

REFERENCES

Ang, A. L., Folsch, H., Koivisto, U. M., Pypaert, M., and Mellman, I. (2003). The Rab8 GTPase selectively regulates AP-1B-dependent basolateral transport in polarized Madin-Darby canine kidney cells. J. Cell Biol. *163*, 339–350.

Braun, A., Pinyol, R., Dahlhaus, R., Koch, D., Fonarev, P., Grant, B. D., Kessels, M. M., and Qualmann, B. (2005). EHD proteins associate with syndapin I and II and such interactions play a crucial role in endosomal recycling. Mol. Biol. Cell *16*, 3642–3658.

Caplan, S., Naslavsky, N., Hartnell, L. M., Lodge, R., Polishchuk, R. S., Donaldson, J. G., and Bonifacino, J. S. (2002). A tubular EHD1-containing compartment involved in the recycling of major histocompatibility complex class I molecules to the plasma membrane. EMBO J. *21*, 2557–2567.

Conner, S. D., and Schmid, S. L. (2003). Regulated portals of entry into the cell. Nature *422*, 37–44.

Daumke, O., Lundmark, R., Vallis, Y., Martens, S., Butler, P. J., and McMahon, H. T. (2007). Architectural and mechanistic insights into an EHD ATPase involved in membrane remodelling. Nature *449*, 923–927.

Fischer, J., Weide, T., and Barnekow, A. (2005). The MICAL proteins and rab1, a possible link to the cytoskeleton? Biochem. Biophys. Res. Commun. *328*, 415–423.

Fukuda, M., Kanno, E., Ishibashi, K., and Itoh, T. (2008). Large scale screening for novel rab effectors reveals unexpected broad Rab binding specificity. Mol. Cell Proteom. *7*, 1031–1042.

George, M., Ying, G., Rainey, M. A., Solomon, A., Parikh, P. T., Gao, Q., Band, V., and Band, H. (2007). Shared as well as distinct roles of EHD proteins revealed by biochemical and functional comparisons in mammalian cells and *C. elegans*. BMC Cell Biol. *8*, 3.

Grant, B., Zhang, Y., Paupard, M. C., Lin, S. X., Hall, D. H., and Hirsh, D. (2001). Evidence that RME-1, a conserved *C. elegans* EH-domain protein, functions in endocytic recycling. Nat. Cell Biol. *3*, 573–579.

Grant, B. D., and Caplan, S. (2008). Mechanisms of EHD/RME-1 protein function in endocytic transport. Traffic *9*, 2043–2052.

Grosshans, B. L., Ortiz, D., and Novick, P. (2006). Rabs and their effectors: achieving specificity in membrane traffic. Proc. Natl. Acad. Sci. USA *103*, 11821–11827.

Hattula, K., Furuhjelm, J., Tikkanen, J., Tanhuanpaa, K., Laakkonen, P., and Peranen, J. (2006). Characterization of the Rab8-specific membrane traffic route linked to protrusion formation. J. Cell Sci. *119*, 4866–4877.

Henry, L., and Sheff, D. R. (2008). Rab8 regulates basolateral secretory, but not recycling, traffic at the recycling endosome. Mol. Biol. Cell *19*, 2059–2068.

Hopkins, C. R. (1983). Intracellular routing of transferrin and transferrin receptors in epidermoid carcinoma A431 cells. Cell *35*, 321–330.

Huber, L. A., Pimplikar, S., Parton, R. G., Virta, H., Zerial, M., and Simons, K. (1993). Rab8, a small GTPase involved in vesicular traffic between the TGN and the basolateral plasma membrane. J. Cell Biol. *123*, 35–45.

Jovic, M., Kieken, F., Naslavsky, N., Sorgen, P. L., and Caplan, S. (2009). Eps15 homology domain 1-associated tubules contain phosphatidylinositol-4-phosphate and phosphatidylinositol-(4,5)-bisphosphate and are required for efficient recycling. Mol. Biol. Cell *20*, 2731–2743.

Jovic, M., Naslavsky, N., Rapaport, D., Horowitz, M., and Caplan, S. (2007). EHD1 regulates beta1 integrin endosomal transport: effects on focal adhesions, cell spreading and migration. J. Cell Sci. *120*, 802–814.

Lee, D. W., Zhao, X., Scarselletta, S., Schweinsberg, P. J., Eisenberg, E., Grant, B. D., and Greene, L. E. (2005). ATP Binding regulates oligomerization and endosome association of RME-1 family proteins. J. Biol. Chem. *280*, 280–290.

Lin, S. X., Grant, B., Hirsh, D., and Maxfield, F. R. (2001). Rme-1 regulates the distribution and function of the endocytic recycling compartment in mammalian cells. Nat. Cell Biol. *3*, 567–572.

Linder, M. D., Uronen, R. L., Holtta-Vuori, M., van der Sluijs, P., Peranen, J., and Ikonen, E. (2006). Rab8-dependent recycling promotes endosomal cholesterol removal in normal and sphingolipidosis cells. Mol. Biol. Cell. *18*, 47–56.

Maxfield, F. R., and McGraw, T. E. (2004). Endocytic recycling. Nat. Rev. Mol. Cell Biol. *5*, 121–132.

Mayor, S., and Pagano, R. E. (2007). Pathways of clathrin-independent endocytosis. Nat. Rev. Mol. Cell Biol. *8*, 603–612.

Naslavsky, N., Boehm, M., Backlund, P. S., Jr., and Caplan, S. (2004). Rabenosyn-5 and EHD1 Interact and Sequentially Regulate Protein Recycling to the Plasma Membrane. Mol. Biol. Cell *15*, 2410–2422.

Naslavsky, N., and Caplan, S. (2005). C-terminal EH-domain-containing proteins: consensus for a role in endocytic trafficking, EH? J. Cell Sci. *118*, 4093–4101.

Naslavsky, N., Rahajeng, J., Chenavas, S., Sorgen, P. L., and Caplan, S. (2007). EHD1 and Eps15 interact with phosphatidylinositols via their Eps15 homology domains. J. Biol. Chem. *282*, 16612–16622.

Naslavsky, N., Rahajeng, J., Sharma, M., Jovic, M., and Caplan, S. (2006). Interactions between EHD proteins and Rab11-FIP2, a role for EHD3 in early endosomal transport. Mol. Biol. Cell *17*, 163–177.

Naslavsky, N., Weigert, R., and Donaldson, J. G. (2003). Convergence of non-clathrin- and clathrin-derived endosomes involves Arf6 inactivation and changes in phosphoinositides. Mol. Biol. Cell *14*, 417–431.

Nishimura, N., and Sasaki, T. (2008). Regulation of epithelial cell adhesion and repulsion: role of endocytic recycling. J. Med. Invest. *55*, 9–16.

Pfeffer, S., and Aivazian, D. (2004). Targeting Rab GTPases to distinct membrane compartments. Nat. Rev. Mol. Cell Biol. *5*, 886–896.

Rapaport, D., Auerbach, W., Naslavsky, N., Pasmanik-Chor, M., Galperin, E., Fein, A., Caplan, S., Joyner, A. L., and Horowitz, M. (2006). Recycling to the plasma membrane is delayed in EHD1 knockout mice. Traffic *7*, 52–60.

Roland, J. T., Kenworthy, A. K., Peranen, J., Caplan, S., and Goldenring, J. R. (2007). Myosin Vb interacts with Rab8a on a tubular network containing EHD1 and EHD3. Mol. Biol. Cell *18*, 2828–2837.

Sharma, M., Jovic, M., Kieken, F., Naslavsky, N., Sorgen, P. L., and Caplan, S. (2009). A model for the role of EHD1-containing membrane tubules in endocytic recycling. Commun. Integr. Biol. *2*, 431–433.

Sharma, M., Naslavsky, N., and Caplan, S. (2008). A role for EHD4 in the regulation of early endosomal transport. Traffic *9*, 995–1018.

Suzuki, T., Nakamoto, T., Ogawa, S., Seo, S., Matsumura, T., Tachibana, K., Morimoto, C., and Hirai, H. (2002). MICAL, a novel CasL interacting molecule, associates with vimentin. J. Biol. Chem. *277*, 14933–14941.

Terai, T., Nishimura, N., Kanda, I., Yasui, N., and Sasaki, T. (2006). JRAB/MICAL-L2 is a junctional Rab13-binding protein mediating the endocytic recycling of occludin. Mol. Biol. Cell *17*, 2465–2475.

Weide, T., Teuber, J., Bayer, M., and Barnekow, A. (2003). MICAL-1 isoforms, novel rab1 interacting proteins. Biochem. Biophys. Res. Commun. *306*, 79–86.

Xu, Y., Shi, H., Wei, S., Wong, S. H., and Hong, W. (2004). Mutually exclusive interactions of EHD1 with GS32 and Syndapin II. Mol. Membr. Biol. *21*, 269–277.

Yamamura, R., Nishimura, N., Nakatsuji, H., Arase, S., and Sasaki, T. (2008). The interaction of JRAB/MICAL-L2 with Rab8 and Rab13 coordinates the assembly of tight junctions and adherens junctions. Mol. Biol. Cell *19*, 971–983.